



## Discontinuity in Jupiter's main auroral oval

A. Radioti,<sup>1</sup> J.-C. Gérard,<sup>1</sup> D. Grodent,<sup>1</sup> B. Bonfond,<sup>1</sup> N. Krupp,<sup>2</sup> and J. Woch<sup>2</sup>

Received 27 June 2007; revised 11 September 2007; accepted 10 October 2007; published 30 January 2008.

[1] On the basis of a series of FUV Hubble Space Telescope images obtained between 1997 and 2007 it is shown that there is a segment of the main auroral oval where the emission drops significantly from a few hundreds to a few tens of kiloRayleigh, forming a discontinuity in the oval. It is shown that the discontinuity is present in both hemispheres and confined in magnetic local time. Its equatorial source is located in the prenoon and early noon sector. The main auroral oval is associated with the ionosphere-magnetosphere coupling current system which is related to the breakdown of corotation in the middle magnetosphere. Necessary for the electron precipitation in the ionosphere and the formation of the main auroral oval is the presence of upward field-aligned currents, carried by downward moving electrons. Field-aligned currents inferred by Pioneer, Voyager and Galileo in situ observations in the near equatorial plane showed evidence of reduced or/and downward field-aligned currents in the prenoon and early afternoon sector, the location of the equatorial source of the discontinuity. Additionally, we estimate the precipitation energy flux in the ionosphere, for a typical reduced upward field-aligned current value at that region, which is found to be within the range of the observed brightness of the discontinuity. Field aligned current distributions in the ionosphere based on magnetohydrodynamic simulations of the interaction between the solar wind and the magnetosphere have predicted a region of downward currents implying a discontinuity at the main auroral oval emission, in very good agreement with the HST observations presented in this work.

**Citation:** Radioti, A., J.-C. Gérard, D. Grodent, B. Bonfond, N. Krupp, and J. Woch (2008), Discontinuity in Jupiter's main auroral oval, *J. Geophys. Res.*, 113, A01215, doi:10.1029/2007JA012610.

### 1. Introduction

[2] Analysis of Hubble Space Telescope (HST) ultraviolet images has shown that Jupiter's auroral emissions, according to their locations, physical regions, precipitation processes [Grodent *et al.*, 2003a, 2003b] and time variations [Clarke *et al.*, 1998] are divided into three main regions. With increasing latitude these three regions, indicated in Figure 1, are: the satellite footprints, the main oval and the polar emissions. The satellite footprints together with their trailing tails are magnetically connected to the orbits of the moons Io, Europa and Ganymede and therefore easy to identify [Clarke *et al.*, 2002a; Grodent *et al.*, 2006; Gérard *et al.*, 2006; Bonfond *et al.*, 2007]. The polar emissions, located poleward of the main oval are magnetically connected to the outer magnetosphere and open field lines [Cowley *et al.*, 2003b; Grodent *et al.*, 2003b]. Their morphology and brightness show large variations on time-scales ranging from seconds to days [Grodent *et al.*, 2003b] and in some cases particular structures such as bright flares are observed [Waite *et al.*, 2001].

[3] The main auroral oval forms a relative stable strip of emission around the magnetic pole. Observations of the main oval emissions demonstrated that they corotate with the planet [Gérard *et al.*, 1994; Ballester *et al.*, 1996] and they show temporal variations on timescales of tens of minutes and hours. Grodent *et al.* [2003a] performed a long term comparison of HST images and showed that the auroral morphology is fixed in system-III longitude (SIII). They produced a reference oval for comparison with images taken on different days, which is used later in this work. The main auroral oval emission [Grodent *et al.*, 2003a] is estimated to contribute to ~75% of the Jovian auroral brightness integrated over the pole and its brightness was shown to vary between 50 and 500 kR (with a few exceptions where the main oval brightened up to 1 MR). Furthermore a statistical analysis of the main oval as a function of CML (Central Meridian Longitude in SIII) exhibits a modulation of the brightness which, for some sectors increases from noon to dusk and then decreases again in the magnetic evening [Grodent *et al.*, 2003a]. A recent study of the morphology of the main aurora emissions [Grodent *et al.*, 2008] reveals several individual details of the main oval in terms of local time: the dawnside portion forms a relatively narrow arc, appearing almost continuous in UV images, the post-noon portion consists of auroral patches and the dusk portion appears to broaden and break from the main oval. These recent observations

<sup>1</sup>LPAP, Institut d'Astrophysique et de Géophysique, Université de Liège, Belgium.

<sup>2</sup>Max-Planck-Institut für Sonnensystemforschung, Katlenburg-Lindau, Germany.

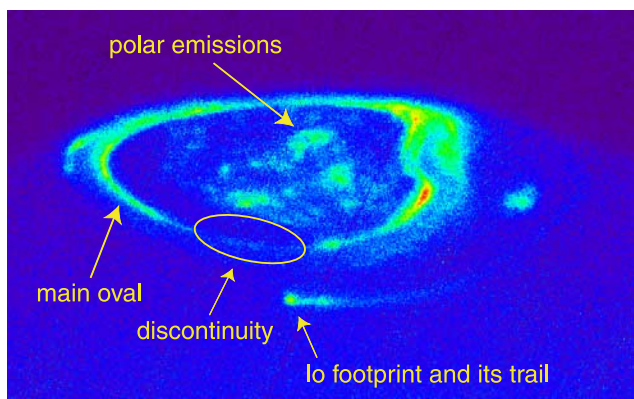


**Figure 1.** Raw HST-STIS clear image showing the FUV auroral emission at the north pole of Jupiter, taken on 28 December 2000. The CML is  $153^\circ$ . The arrows indicate the main auroral features: the main oval, the Io footprint and its trail and the polar emissions. The ellipse indicates the discontinuity in the main oval.

suggest substitution of the term “main oval”, which was initially used to describe the Earth auroral emissions, with the term “main emission”. In this study the term “main oval” will be often used to describe the term “main emission”.

[4] Theoretical studies suggest that the main Jovian auroral oval is connected to the magnetosphere-ionosphere coupling current system associated with the breakdown of rigid corotation in the middle magnetosphere and maps to the equatorial plane between  $\sim 15$  and  $\sim 40 R_J$  [Cowley and Bunce, 2001; Hill, 2001; Southwood and Kivelson, 2001; Nichols and Cowley, 2004]. As the plasma diffuses outwards in the equatorial plane its angular velocity decreases due to conservation of the angular momentum. At a certain distance, breakdown of corotation occurs and a strong current system develops. When the plasma angular velocity becomes lower than that of the neutral atmosphere ion-neutral collisions occur in the Pedersen layer of the ionosphere. These produce a frictional torque which tends to spin the plasma back up toward corotation with the planet. The current circuit is closed by a system of field-aligned currents which flow from the ionosphere to the equator (upward) in the inner part of the system, and return (downward) in the outer part. The upward field aligned currents which are carried by downward moving electrons are associated with the main auroral oval. In this study we concentrate in the description of the field aligned currents since they are necessary for the formation of the main auroral oval emissions. However, it is shown that other auroral emissions can occur without the need of field-aligned currents, such as diffuse emissions by electron scattering [Bhattacharya et al., 2001] and secondary oval emissions by electron pitch angle scattering due to whistler waves [Tomás et al., 2004].

[5] Field-aligned current calculations are inferred from in situ observations. Bunce and Cowley [2001b] used Pioneer and Voyager measurements in the middle magnetosphere (20 to  $50 R_J$ ) and found upward currents in the postmidnight sector along the Voyager passes and downward currents in the dawn ( $\sim 04:30$  LT) and prenoon ( $\sim 09:00$  LT) sector

along the Pioneer trajectories. On the basis of Galileo magnetic field observations Khurana [2001] calculated field-aligned current distributions in the near equatorial plane. He showed the existence of upward currents in an arc from  $\sim 13:00$  to  $\sim 08:00$  LT and downward currents from  $\sim 08:00$  to  $\sim 13:00$  LT. Apart from observations, simulations have also predicted equatorial and ionospheric distributions of field-aligned currents. Walker and Ogino [2003] used a global magnetohydrodynamic simulation based on the interaction of Jupiter’s magnetosphere with the solar wind, and produced field-aligned current distributions in the near equatorial magnetosphere. The equatorial field-aligned current pattern revealed upward currents in all local time sectors except in the late morning and early afternoon, in agreement with the observations. Additionally, the same authors mapped the currents along magnetic field lines from the equatorial plane to the ionosphere for various solar wind conditions.

[6] Estimations of the field-aligned currents [Cowley and Bunce, 2001] suggest the existence of field-aligned voltages of the order of  $\sim 100$  kV responsible for the acceleration of primary auroral electrons to  $\sim 100$  keV, able to produce the brightness of the observed main auroral emissions and the mean electron energy deduced from the UV spectral analyses [Gustin et al., 2004]. However, theoretical considerations [Cowley and Bunce, 2001, 2003; Cowley et al., 2003a, 2005] suggested that the aurora intensity is regulated by the extent to which the equatorial plasma departs from rigid corotation, with the largest coupling currents and the most intense auroras being associated with the largest departures. Krupp et al. [2001] reported measurements of plasma flow velocities in the equatorial plane. They derived a global flow pattern in the magnetosphere of Jupiter, based on directional anisotropies of energetic ion distributions by the Energetic Particles Detector onboard Galileo. They showed that the flow is predominately directed in the corotation direction. Strong dawn-dusk asymmetry is evident in the plasma flow: the nearly corotating ions in the dawn-to-noon quadrant suddenly slow down in the noon-to-dusk quadrant.

[7] In this work we make use of the VIP4 magnetic model [Connerney et al., 1998], constrained from in situ magnetic field measurements and remote observations of the position of the foot of Io flux tube in Jupiter’s ionosphere. Grodent et al. [2003a] compared the reference ovals in the north and south with the footprints of the magnetic field lines of  $30 R_J$  as derived by the VIP4 model [see Grodent et al., 2003a, Figure 6]. The observed and the VIP4 ovals are in relatively good agreement, especially for the southern hemisphere. However, localized deviations do occur, with the larger inconsistencies in the northern hemisphere. The main oval reference deviates from the  $30 R_J$  oval between the  $190^\circ$  and  $230^\circ$  meridians and the inconsistency is amplified along the  $150^\circ$  meridian in a region called the “kink” that is speculated to be the result of an internal magnetic anomaly [Clarke et al., 2002b; Grodent et al., 2003a]. The deviations could also come from the fact that the main oval connects emission features that may very well map to different regions of the magnetosphere and it should not be assumed to be at a fixed radial distance footprint. Additionally, recent studies, making use of the VIP4 magnetic field model, showed that the latitudinal variations of the main oval

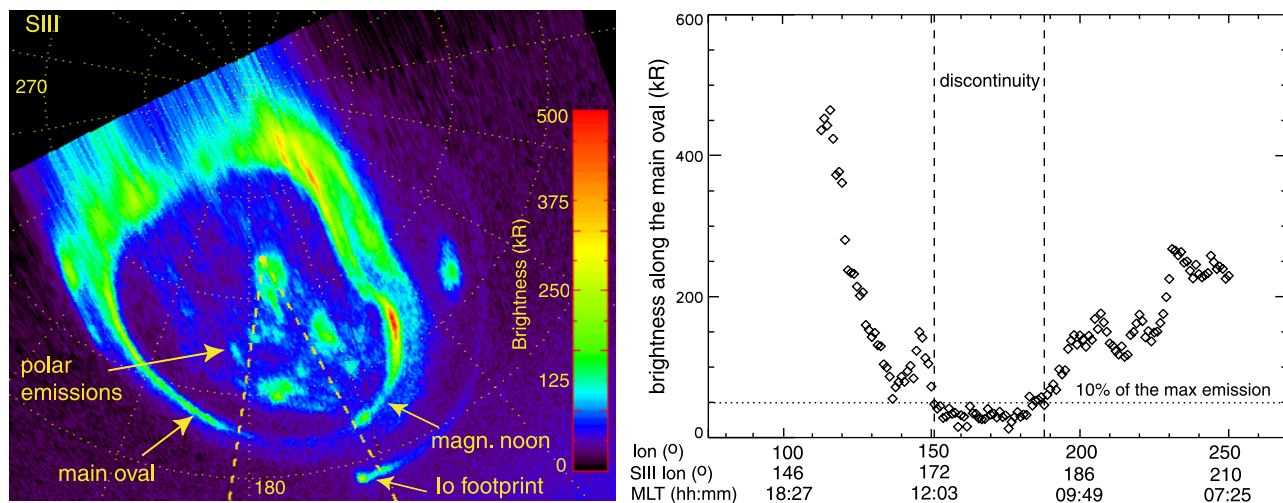


**Figure 2.** Left panel: Polar projection of an aurora image in System III polar coordinate system (dots) taken by HST-STIS on 28 December 2000 in the north hemisphere. The CML is  $153^\circ$ . The circle indicates the morphological center of the main oval ( $\lambda = 185^\circ$  and  $\phi = 74^\circ$ ) [Grodent *et al.*, 2004]. The dashed lines show the meridians starting from the center and define the position of the discontinuity. The main auroral features and the magnetic noon are indicated. The raw image is shown in Figure 1. The color scale shows the brightness in kR. Note that in deriving the brightness the limb brightening effect is not taken into account. Right panel: Brightness profile of the main oval in kR (above the background emission), as a function of the longitude (deg) of meridians with respect to the morphological center of the main oval, the longitude in SIII (deg) and the magnetic local time (hh:mm) derived by the magnetic field model VIP4. The horizontal dotted line indicates the threshold of 10% of the maximum brightness along the main oval and the vertical dashed lines show the boundaries of the discontinuity.

location could be the result of internal variation of the current sheet parameters [Grodent *et al.*, 2008].

[8] In the present study we will concentrate on a region of the main oval close to magnetic noon, where a clear drop of the intensity is frequently observed. In the first part, examples of the observed discontinuity for the north and south hemispheres are shown, followed by statistical results and the determination of its location in the equatorial plane. In the second part, observations, theoretical considerations and simulations of the field-aligned currents in the Jovian magnetosphere are discussed in association with the observed discontinuity.

## 2. HST Observations of the Discontinuity in Jupiter's Main Auroral Oval

### 2.1. Data Reduction

[9] In this work we analyze images that were taken with the photon-counting detector MAMA (MultiAnode Micro Channels Array) of the STIS (Space Telescope Imaging Spectrograph) and ACS (Advanced Camera of Survey) on board the Hubble Space Telescope (HST). The MAMA array consists of  $1024 \times 1024$  pixels providing a field of view (FOV) of  $24.7'' \times 24.7''$  with a  $\sim 0.08''$  full width at half maximum point spread function (PSF). Four different filters are used: clear and SrF2 from STIS and F115LP and F125LP from ACS. The brightness derived in this paper considers a conversion factor of count per pixel per second for 1 kiloRayleigh (kR) of  $H_2$  emission plus Lyman- $\alpha$  different for each filter. In particular, a factor of 0.0015, 0.0005, 0.0049 and 0.00347 is used for clear, SrF2, F115LP and F125LP filters, respectively. In the image processing is

not taken into account the limb brightening effect. So as to project the images a limb-fitting procedure is needed to determine the center position of the planet. By this procedure the initial image is projected on a SIII map on which features corotating with planet, leading or lagging corotation are easy to detect. However, in this method there is a growing uncertainty toward the limb and the pixels are stretched. For a detailed description of the data set and data reduction see Grodent *et al.* [2003a].

[10] The viewing geometry for the southern Jovian aurora is less favorable for the Earth-based observations. The vicinity of the magnetic south pole to the rotation axis restricts the view of the southern aurora compared to the northern. The stretching of the southern aurora emission near the limb persists and the location of the auroral emission in the south remains less accurate. Therefore we emphasize more the analysis of images in the northern hemisphere.

### 2.2. Discontinuity in the Main Auroral Oval: Observations

[11] Figure 1 shows an HST-STIS image of the FUV auroral emission at the north pole of Jupiter. The three main auroral features: the main oval, the Io footprint together with its trail and the polar emissions poleward of the main oval are indicated by the arrows. In this study we concentrate on a region along the main oval where the brightness drops forming a discontinuity. The location of this discontinuity is marked by the ellipse in Figure 1.

[12] We view the aurora image in a polar projection in system III polar coordinate system, where features that corotate, lead or lag corotation are easy to detect. Figure 2,

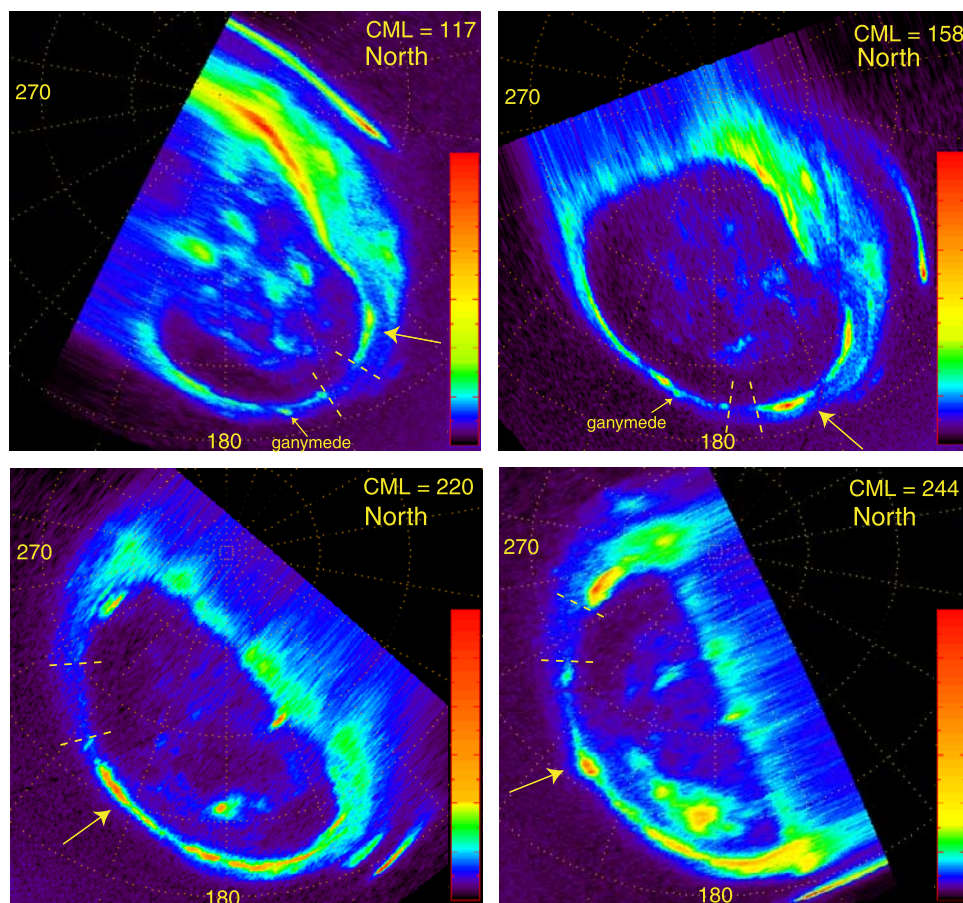


**Figure 3.** Polar projections of 4 HST STIS images in the north hemisphere in system III polar coordinate system. The images are taken at the same day, 16 December 2000, at different CML. The arrows show the magnetic noon and the dashed lines perpendicular to the main oval show the edges of the discontinuity. Ganymede footprints are indicated in the top panels. The color bars in each panel indicate the brightness emission with maximum at the top and minimum at the bottom of the scale.

left panel shows a polar projection in SIII of the image taken on 28 December 2000 in the north Jovian hemisphere. The CML is  $153^\circ$  and the color bar indicates the brightness in kR. The main auroral features and the magnetic noon are indicated. The circle in the center of the auroral emission shows its morphological center of the main oval, which is located in SIII longitude  $\lambda = 185^\circ$  and latitude  $\phi = 74^\circ$  [Grodent *et al.*, 2004]. The morphological center is derived geometrically and it is independent of any magnetic field model. From the morphological center we draw meridian cuts along which we measure the emission of the main oval. The meridians between which the discontinuity is observed are indicated by the dashed lines. The right panel of Figure 2 shows the brightness profile above the background emission along the main oval as a function of longitude with respect to the morphological center. The associated SIII longitude (deg) as well as the magnetic local time, MLT (hh:mm), derived by the magnetic field model VIP4 are shown for reference. It is evident that the brightness drops and remains low for several tens of degrees in the prenoon local time sector. We define the discontinuity as the region along the main oval, where the emission drops below 10% of the maximum emission of the visible portion of the main oval. The “10%” boundary is set empirically to represent

the drop of the emission along the oval. The same criterion is used for all the images examined in this study. When the emission near the discontinuity is changing less abruptly an uncertainty in defining the boundary of the discontinuity can appear. This is in the order of a few degrees which corresponds to a few tens of minutes in MLT. For example a deviation of 5 deg will change the location of the discontinuity in MLT by 10 to 30 min depending on its SIII position.

[13] We locate the discontinuity in the main oval in other aurora images, based on the same method. We analyze HST images taken on the same day but at different CML, in order to examine the origin of the discontinuity. Figure 3 shows aurora polar projections in SIII taken on 16 December 2000 at different CML in the northern hemisphere. The arrows indicate the magnetic noon and the dashed lines perpendicular to the main oval the edges of the discontinuity, derived the same way as described in Figure 2. It is evident that the discontinuity is not observed in a fixed position in SIII. However, it appears fixed in magnetic local time, between the prenoon and noon sector. The width of the discontinuity is shown to vary from image to image, as it is revealed by the statistical study below (Table 1). On the top panels of

**Table 1.** Statistical Analyses of the Discontinuity in Jupiter's Main Auroral Oval Based on 56 Images

	Range	Mean Value
Width, <sup>a,b</sup> deg	0–110	35
Minimum emission, kR	5–95	34
Local time, <sup>c</sup> h	06:00–13:00	~10:00

<sup>a</sup>The meridians are traced from the morphological center.

<sup>b</sup> $\pm 5^\circ$  due to the uncertainty in defining the discontinuity.

<sup>c</sup> $\pm 30$  min due to the uncertainty in defining the discontinuity.

the same figure the Ganymede footprint is indicated. It appears close to the discontinuity and slightly equatorward. It will be later used as reference for mapping the discontinuity to the equatorial plane. Ganymede footprints at the two bottom images could not be identified.

[14] It is necessary to map the position of the discontinuity to the equatorial plane in order to investigate the equatorial source of this feature. The left panel of Figure 4 is a summary plot of the position of the discontinuity based on Figure 3. The locations of the discontinuity for different CML are plotted with different symbols on top of a reference oval [Grodent *et al.*, 2003a] on a polar projection in SIII. The filled symbols indicate the Ganymede footprint which is located next to the discontinuity. It is shown that the location of the discontinuity is not favoring a specific SIII longitude and it can appear along different parts of the main oval. We magnetically map the position of the discontinuity from the ionosphere to the equatorial plane, making use of the VIP4 magnetic field model (right panel

of Figure 4). The equatorial source of the discontinuity is concentrated in the prenoon magnetic local time sector between 10 and 20  $R_J$ . However, theoretical predictions locate the breakdown of corotation responsible for the main oval emission between 15 and 40  $R_J$ . The reason for the inconsistency stems from the fact that especially in the northern hemisphere the 30  $R_J$  oval derived by VIP4 magnetic field model deviates from the observed reference oval [Grodent *et al.*, 2003a]. Such an inconsistency can be attributed to various reasons. VIP4 is constrained by observations of the Io footprint and might be inaccurate at distance larger than 5.9  $R_J$  (Io orbit). Additionally, the main oval maps to equatorial regions ranging between 15  $R_J$  and several tens of  $R_J$  and should not be assumed to be at a fixed radial distance footprint. Recent studies also showed that latitudinal variations of the main oval location do exist and could be the result of internal variation of the current sheet parameters [Grodent *et al.*, 2008]. The reasons above could justify the fact that the equatorial source of the discontinuity at the main oval, shown in Figure 4 deviates from the 15 to 40  $R_J$ , the theoretically predicted equatorial origin of the main oval.

[15] The satellite footprints, since they are magnetically connected to the moons could serve as absolute reference points for the magnetic mapping from the ionosphere to the equatorial plane. The Ganymede footprints next to the position of the discontinuity and slightly equatorward are marked on the left panel in Figure 4 with the filled symbols. They are magnetically connected to 15  $R_J$ , implying that the position of the discontinuity is located slightly further than

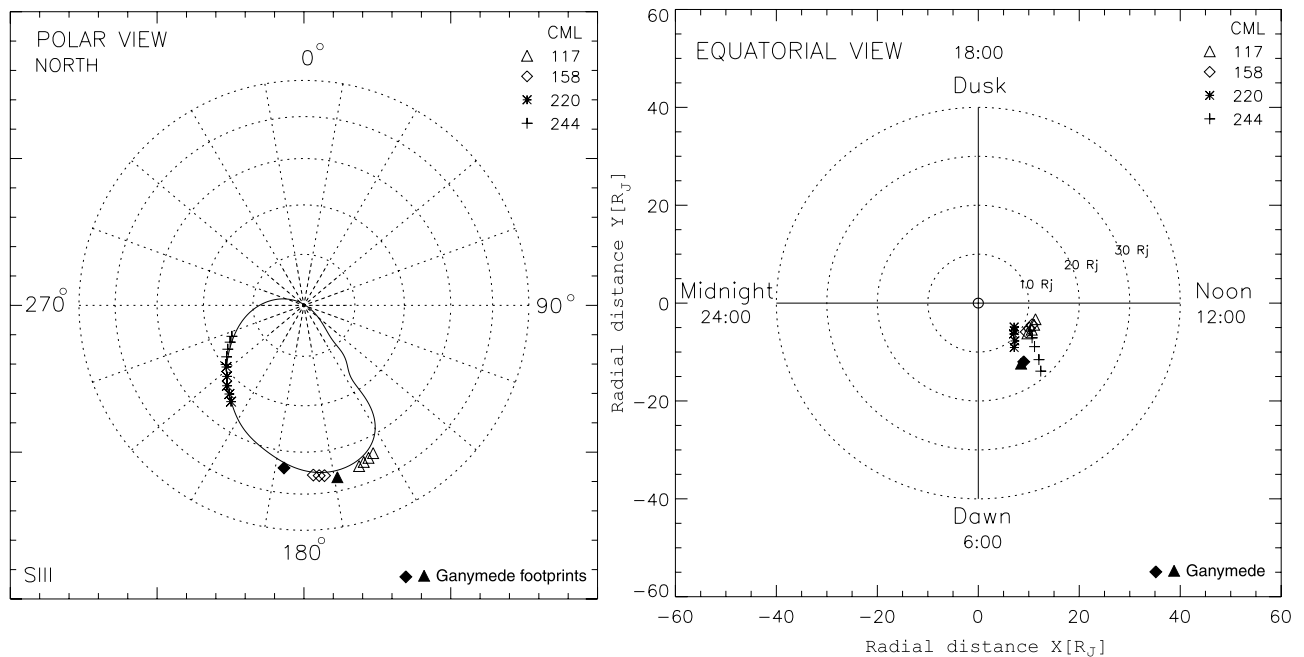


**Figure 4.** Left panel: Polar view in SIII of the position of the discontinuity for the images in Figure 4 taken on the 16 December 2000 at the north hemisphere. The different symbols correspond to the position of the discontinuity at different CML. The filled symbols indicate the position of the Ganymede footprint based on Figure 3. A reference main oval [Grodent *et al.*, 2003a] is shown by the solid line. Right panel: The position of the discontinuity on the equatorial plane with the Sun to the right. The filled symbols indicate the position of Ganymede on the equatorial plane. For the magnetic mapping from the ionosphere to the equatorial plane the magnetic field model VIP4 [Connerney *et al.*, 1998] is used.

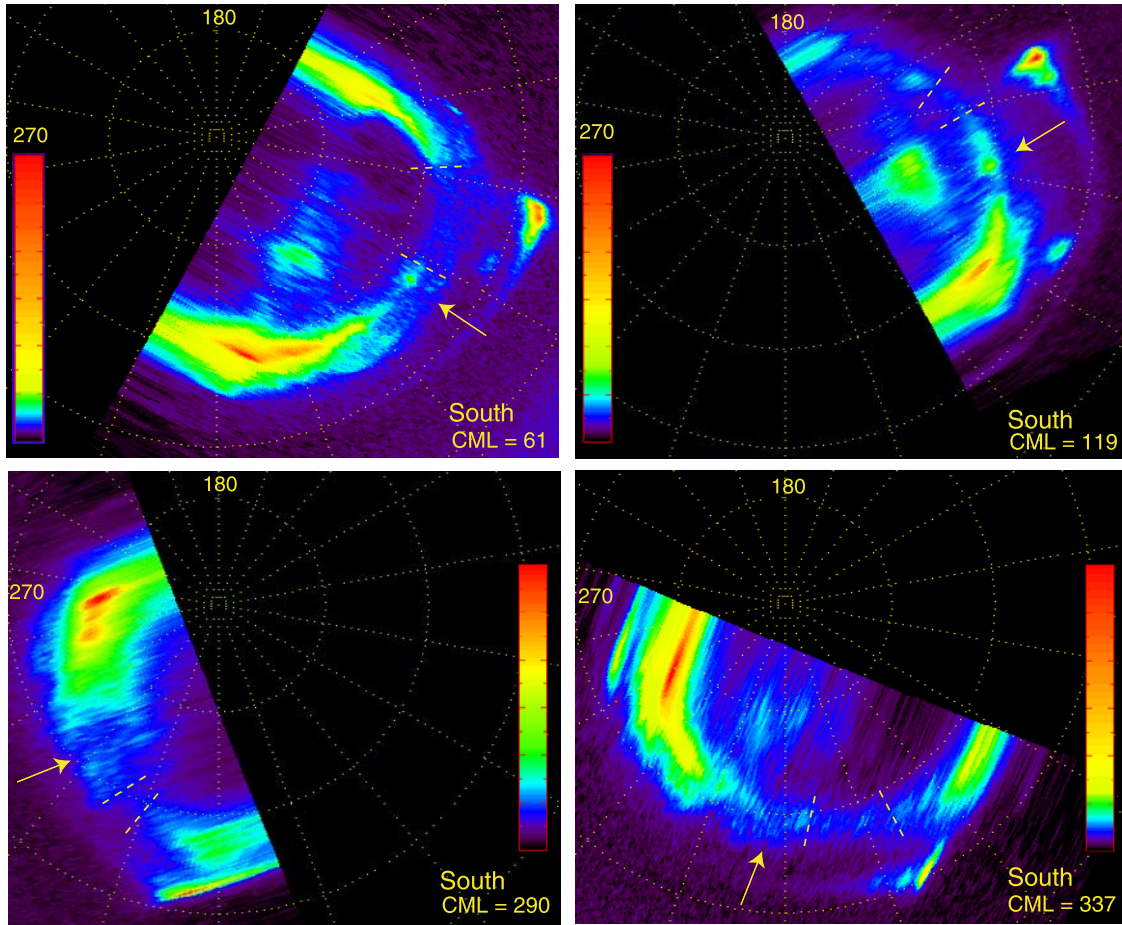


**Figure 5.** Polar projections of 4 HST STIS images on the south hemisphere in system III polar coordinate system. The images are taken at the same day, on the 28 December 2000, at different CML. The arrows show the magnetic noon and the dashed lines perpendicular to the main oval show the edges of the discontinuity. The color bars in each panel indicate the brightness emission with maximum at the top and minimum at the bottom of the scale.

15  $R_J$ . On the right panel of Figure 4 the position of Ganymede for both CML is indicated, for reference, on the equatorial plane.

[16] Similar analysis has been performed for the emissions in the south hemisphere. Figure 5 shows polar projections of aurora images in SIII on the south hemisphere. The images are taken by the HST-STIS telescope on 28 December 2000 along the same day but at different CML. The position of the discontinuity in the southern images is derived the same way as described in Figure 2 and it is indicated by the dashed lines perpendicular to the main oval. It is demonstrated that the discontinuity at the main oval exists in the south and is not observed at a fixed SIII position. We summarize the position of the discontinuity for different CML on a polar view on top of the reference oval in the southern hemisphere (left panel of Figure 6). We map its position from the ionosphere to the equatorial plane as it is shown in the right panel of the same figure. The position of the discontinuity in the south hemisphere appears to be fixed in the prenoon local time sector. It is thus demonstrated that the discontinuity is a feature appearing in both hemispheres and has a common equatorial source region. However, the discontinuity in the south hemisphere maps at

slightly different radial distances (20–30  $R_J$ ) than those in the north (10–20  $R_J$ ) shown in the right panel of Figure 4. The discrepancies come from the fact that the deviation of the 30  $R_J$  oval derived by the VIP4 magnetic field model and the observed reference oval [Grodent *et al.*, 2003a] is much larger in the north than in the south hemisphere. Possible reasons for this inconsistency are mentioned in the introduction.

[17] Additionally, a statistical analysis is performed for the north hemisphere where the coverage is larger. 64 STIS and ACS images are analyzed during the years 1997–2007, one for each day available. Table 1 summarizes some parameters characterizing the discontinuity based on the statistical study. 56 out of 64 images show a discontinuity in the main oval emission. The minimum emission that is observed along the discontinuity ranges between 5 and 95 kR with a mean minimum brightness of  $\sim 34$  kR. The width of the discontinuity is mostly less than  $40^\circ$  (mean width  $\sim 35^\circ$ ) with a few exceptions up to  $110^\circ$ . To these values an uncertainty of  $\pm 5^\circ$  is added, coming from the inaccuracy in defining the discontinuity. The width of the discontinuity is measured by the meridians traced from the morphological center of the main oval (longitude in

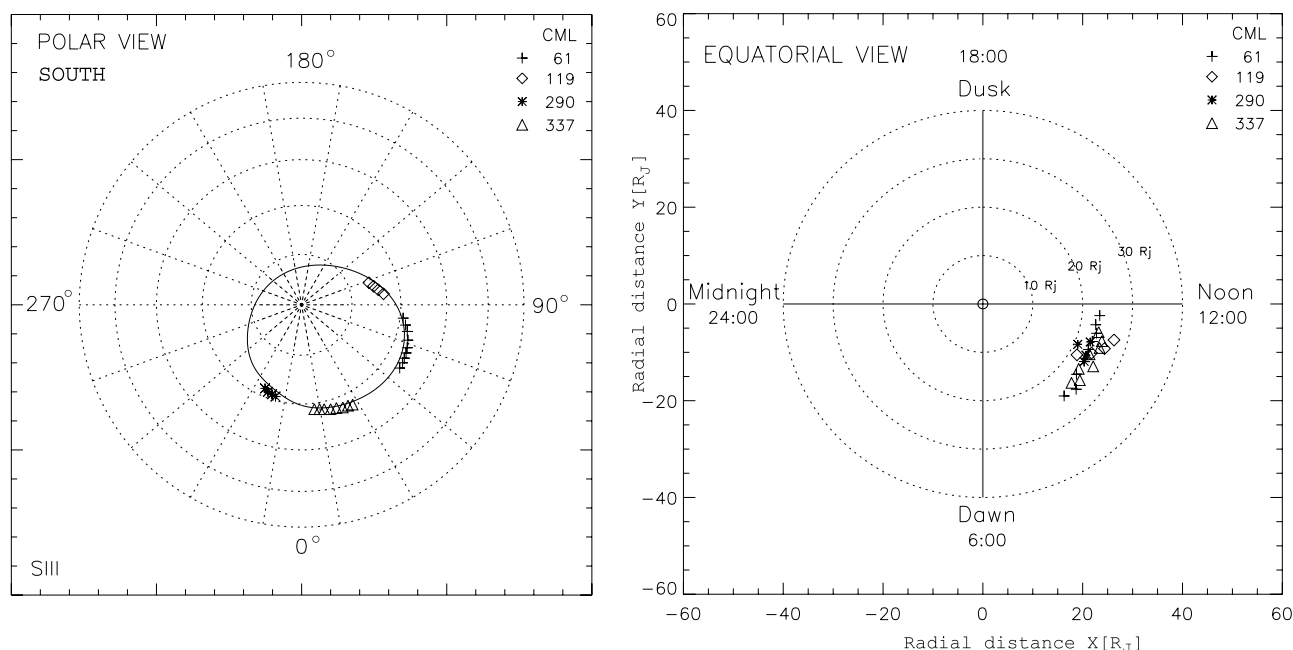


**Figure 6.** Left panel: Polar view in SIII of the position of the discontinuity for the images at Figure 6 taken on the 28 December 2000 at the south hemisphere. A reference main oval [Grodent *et al.*, 2003a] is shown by the solid line. Right panel: The position of the source of the discontinuity on the equatorial plane with the sun to the right. For the magnetic mapping from the ionosphere to the equatorial plane VIP4 [Connerney *et al.*, 1998] is used. The position of the discontinuity at different CML is shown by different symbols in the both panels.

SIII  $\lambda = 185^\circ$  and latitude  $\phi = 74^\circ$ ). One of the most interesting results of the statistical study is the location of the discontinuity in the equatorial plane. The result of the study is shown in the histogram in Figure 7. It is evident that the position of the discontinuity is localized in the prenoon and early noon sector between 08:00 and 13:00 LT ( $\pm 30$  min, due to the uncertainty in defining the discontinuity) with very few exceptions starting from 06:00 LT. This study establishes the existence of the discontinuity at the main auroral oval as a frequently observed feature, with an equatorial source region in the prenoon and noon sector mainly between 08:00 and 13:00 LT. In the next section we discuss the origin of this discontinuity.

### 3. Field-Aligned Current Observations and Simulations: Comparison With Aurora Observations

[18] The main auroral oval is formed in the ionosphere by the precipitation of energetic electrons. A requirement for the presence of precipitating electrons since they are carrying a net current, is an upward field-aligned current to flow along the field lines. Downward field-aligned currents will prohibit electron precipitation in the ionosphere and imply the absence of auroral emissions. In this section we compare the equatorial source of the discontinuity with the field-aligned currents estimations based on in situ spacecraft observations. Bunce and Cowley [2001b] found upward currents along the postmidnight outbound trajectories of Voyager 1 and 2 ( $\sim 03:30$  and  $01:00$  LT, respectively) and downward currents along the Pioneer 10 outbound ( $\sim 4:30$  LT) and Pioneer 11 inbound ( $\sim 9:00$  LT) trajectories,

making use of Pioneer and Voyager measurements in the middle magnetosphere (20 to 50  $R_J$ ). In particular, the Pioneer 11 measurements showed current values close to zero at and beyond 25  $R_J$ . The discrepancies between the different trajectories are attributed to the distribution of the azimuthal currents. The azimuthal currents are estimated in previous studies [Bunce and Cowley, 2001a] to be larger on the nightside and decrease continuously toward noon, via dawn. Bunce and Cowley [2001b] showed that for the Pioneer 10 and 11 passes, the divergence of the azimuthal

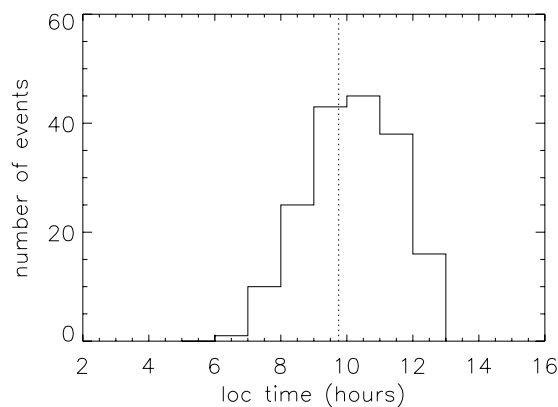


**Figure 7.** Histogram showing the location of the discontinuity in local time. The statistical analysis is based on 56 STIS and ACS images during the years 1997–2007, each of them on a separate day. The dotted line indicates the mean value. The VIP4 magnetic field model [Connerney *et al.*, 1998] is used for the magnetic mapping.

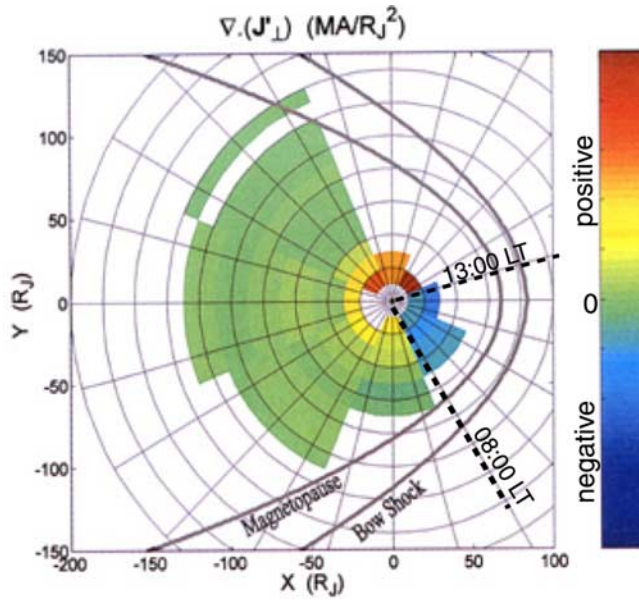


**Figure 8.** Divergence of the height-integrated perpendicular currents ( $\nabla \cdot (\mathbf{J}'_{\perp}) \propto -\mathbf{J}'_{\parallel}$ ) based on Galileo observations and projected on the equatorial plane of Jupiter's magnetosphere [Khurana, 2001]. The locations of the magnetopause and the bow shock are shown. The data are averaged over  $10 R_J \times 3$  h. The warm colors indicate the positive divergence and the cold colors the negative. The dashed lines indicate the starting and ending local times of the discontinuity's position in the equatorial plane 08:00 and 13:00 LT as derived by the statistical analyses.

current is larger than the increase in the radial current suggesting the presence of reversed field-aligned current on their pass flowing from the current sheet to the ionosphere (downward currents). For the Voyager trajectories, however, the azimuthal current can provide only half of the source needed, requiring the formation of upward field-aligned currents. Calculations of the angular velocity profiles (for the same value of Pedersen conductivity,  $\Sigma_p^* = 0.5$  mho) revealed that along the Pioneer passes the angular velocity of the inner part of the region seems to fall less abruptly with distance compared to that along Voyager passes. The authors attributed these discrepancies to magnetospheric dynamics: differing  $I_0$  mass loading rate and compression of the plasma by the magnetopause as it sweeps around from the nightside to the dayside (solar wind induced asymmetry effects). Alternatively, decreasing the conductivity with the equatorial distance could lead to similar velocity profiles for all spacecraft trajectories [Bunce and Cowley, 2001b]. The same authors related it to the reduced and reversed directions of the inferred field-aligned current.

[19] The presence of downward currents estimated along the Pioneer 10 and 11 passes in the prenoon and dawn sector, respectively, would prohibit electron precipitation in the ionosphere and imply discontinuity in Jupiter's main auroral oval. It is worth investigating thoroughly the measurements along the Pioneer 11 outbound trajectory ( $\sim 9:00$  LT) since it lies within the equatorial source of the discontinuity based on HST images (between 08:00 and

13:00 LT, see Figure 7). From the field-aligned current density values along the Pioneer 11 pass, we aim to derive the precipitated energy flux in the ionosphere and compare it with the observed aurora brightness along the discontinuity in Jupiter's main oval. For this purpose we will also use the Voyager measurements for comparison.

[20] The field-aligned current density  $j_{\parallel}/B$  values derived from Voyager varied from  $\sim 2 \times 10^{-13} \text{ Am}^{-2}\text{nT}^{-1}$  (at  $20 R_J$ ) to  $\sim 1 \times 10^{-13} \text{ Am}^{-2}\text{nT}^{-1}$  (at  $50 R_J$ ) while the Pioneer 11 values were less than  $10^{-13} \text{ Am}^{-2}\text{nT}^{-1}$  approaching zero [Bunce and Cowley, 2001b]. From the  $j_{\parallel}/B$  along the Voyager passes Bunce and Cowley [2001b] calculated the precipitating energy flux in the ionosphere, based on Knight's kinetic theory [Knight, 1973] and using plasma measurements by Voyager (plasma density of  $N \sim 0.01 \text{ cm}^{-3}$  and thermal energy of  $W_{th} \sim 2.5 \text{ keV}$ ). Thus the energy flux in the ionosphere was calculated  $E_f \approx 38 \text{ mWm}^{-2}$  and consequently the auroral brightness  $\sim 380 \text{ kR}$ , a typical value for the main oval emissions [Grodent et al., 2003a]. For the Pioneer 11 pass, with  $j_{\parallel}/B < 10^{-13} \text{ Am}^{-2}\text{nT}^{-1}$  we calculate in a similar way the precipitating energy flux in the ionosphere, using however the Voyager density and temperature parameters. The energy flux in the ionosphere is estimated to be  $E_f \approx 1.56 \text{ mWm}^{-2}$ , which corresponds to  $\sim 15 \text{ kR}$ . This brightness value is near the lower limit but within the range of the observed emission along the discontinuity, as revealed by the statistical study (mean value  $34 \text{ kR}$ , see Table 1).

[21] Field-aligned currents are also estimated based on Galileo magnetic field observations covering all local times and larger radial distances. From the divergence of the height-integrated current flowing in the equatorial plane of Jupiter's magnetosphere Khurana [2001] inferred field-aligned current distributions. The field-aligned current  $J_{\parallel}$  is related to the divergence of the height-integrated perpendicular current ( $\nabla \cdot (\mathbf{J}'_{\perp})$ ), by integration of the current continuity equation over the thickness of the current sheet:

$$-2J_{\parallel} \frac{B_Z}{B_L} = \nabla \cdot (\mathbf{J}'_{\perp}) = \nabla \cdot (\mathbf{J}'_{\rho} + \mathbf{J}'_{\phi}), \quad (1)$$

where  $B_Z$  is assumed to remain constant over the thickness of the current sheet and  $B_L$  is the field strength in the lobe just outside the current sheet.  $\mathbf{J}'_{\rho}$  and  $\mathbf{J}'_{\phi}$  are the height-integrated radial and azimuthal currents which are calculated based on magnetic field observations [Khurana, 2001]. It is obvious that a positive current divergence  $\nabla \cdot (\mathbf{J}'_{\perp})$  in the equatorial plane implies a negative field-aligned current,  $J_{\parallel}$  (directed southward in the northern lobe) in other words an upward flowing field-aligned current.

[22] Figure 8 shows the divergence of the height-integrated perpendicular current ( $\nabla \cdot (\mathbf{J}'_{\perp})$ ), based on computations of the  $\mathbf{J}'_{\rho}$  and  $\mathbf{J}'_{\phi}$ , flowing in the equatorial plane of Jupiter's magnetosphere with the sun to the right [Khurana, 2001]. The locations of the magnetopause and bow shock are also indicated. The data are averaged over  $10 R_J \times 3$  h. The warm colors show the positive current divergence, meaning a current flowing into the current sheet from the ionosphere in both hemispheres (upward current). The cold colors indicate the negative current divergence, implying a current flowing out of the sheet toward the ionosphere in both

hemispheres (downward current). At all local times except for the early prenoon and noon sector between 10 and 30  $R_J$  upward field aligned currents (warm colors) are present, along which electrons can precipitate and create auroral emission. However, there is a region between early prenoon and noon that the field-aligned currents are directed downward, prohibiting electron precipitation.

[23] Such a local time asymmetry in the field-aligned current pattern is not surprising. *Khurana* [2001] reported local time variations of  $\mathbf{J}'_\rho$  and  $\mathbf{J}'_\phi$ . Both quantities appear to be strong near midnight and systematically weak toward noon. As a consequence their divergence  $\mathbf{J}'_\rho$  and  $\mathbf{J}'_\phi$  exhibits local time asymmetries. More specific between the radial distances 10 to 30  $R_J$  all local times except for the noon sector have positive radial current divergence ( $\nabla \cdot \mathbf{J}'_\rho$ ) implying that field-aligned currents are flowing into the plasma sheet in this region. Additionally, calculations of the divergence of the azimuthal current ( $\nabla \cdot \mathbf{J}'_\phi$ ) demonstrated a strong dawn-dusk asymmetry, indicating that electric current is drawn from the ionosphere into the equatorial plane in the dusk sector and returned to it in the dawn sector. The author argued that such a current distribution results from the solar wind driven magnetospheric convection. The  $\nabla \cdot (\mathbf{J}'_\rho)$  a combination of the divergence of  $\mathbf{J}'_\phi$  and  $\mathbf{J}'_\rho$  demonstrates accordingly asymmetries leading to downward field-aligned currents in the noon and prenoon sector.

[24] On top of Figure 8 by dashed lines, we show the statistical view of the equatorial source of the discontinuity. The 08:00 and 13:00 LT meridians, drawn by dashed lines, indicate the starting and ending local times of the discontinuity's position in the equatorial plane, based on the histogram in Figure 7. It is evident that the equatorial source region lies at the same local time sector where field-aligned currents are flowing from the ionosphere into the current sheet (downward currents). The presence of downward field-aligned currents implies that electrons can not precipitate in the ionosphere and the main oval emissions are not produced. However, given that the data in Figure 8 are averaged over 10  $R_J \times 3$  h small variations of the current can be canceled out, such as those inferred by Pioneer 11 at 09:00 LT that could produce faint emission along the discontinuity. This is in agreement with the observations along the discontinuity region, where the emission lowers to <10% of the maximum emission and reaches values of  $\sim 34$  kR (see Table 1). Thus the field-aligned current pattern can predict well the observed position of the discontinuity in Jupiter's main auroral oval.

[25] Theoretical studies suggest that the auroral intensity is regulated by the extent to which the equatorial plasma departs from rigid corotation with the largest coupling currents and the most intense auroras related to the largest departures [*Cowley and Bunce*, 2001, 2003; *Cowley et al.*, 2003a, 2005]. Plasma flow measurements based on Galileo observations have shown strong dawn-dusk asymmetries in the plasma flow [*Krupp et al.*, 2001]: between 15 to 40  $R_J$  in the dawn-to-noon sector the plasma is nearly corotating, while it slows down in the noon-to-dusk sector. This would require weaker corotation enforcement currents, weaker/reversed field-aligned currents and consequently fainter aurora emissions in the prenoon magnetic local time. Such a consideration is in accordance with the downward currents

and reduced field-aligned currents observed by Pioneer and Galileo in the prenoon and early noon sector and could account for justifying the faint auroral emission at the main oval. However, a derivation of the precipitated energy flux in the ionosphere from the plasma flow velocities and comparison with the observed aurora brightness is not included in the present work. Such a study would require the knowledge of the equatorial magnetic field, plasma density and ionospheric conductivity as a function of the radial distance and it is outside the scope of this study.

[26] *Walker and Ogino* [2003] used a global magnetohydrodynamic simulation of the interaction of Jupiter's magnetosphere with the solar wind, which created a field-aligned current pattern in the near equatorial magnetosphere. They showed that the currents in the middle magnetosphere are predicted mostly upwards except in the late morning and early afternoon local time sector in agreement with the field-aligned current pattern inferred by Galileo observations [*Khurana*, 2001]. Azimuthal currents simulations [*Walker and Ogino*, 2003] showed an asymmetric current system as a result of the outflowing rotating plasma on the day side, constrained in the magnetopause until it rotates past noon. The asymmetric azimuthal current system requires downward field-aligned currents at dawn and upwards at dusk as discussed by *Bunce and Cowley* [2001b] and could account for the downward field-aligned currents in the prenoon and early afternoon sector, predicted by the simulations. Additionally *Walker and Ogino* [2003] mapped the field-aligned currents just outside their inner boundary (21  $R_J$ ) along magnetic field lines in the ionosphere. Their simulations, for various solar wind conditions, show that a band of upward currents is present at latitudes which correspond to 20–40  $R_J$  at all local times with an exception in the late prenoon sector, in accordance with our observations.

[27] Reversed field-aligned currents at other local times such as those inferred by Pioneer 10 at 04:30 LT [*Bunce and Cowley*, 2001b] are not shown in the average field-aligned current pattern derived from Galileo data and the simulated currents by *Walker and Ogino* [2003]. Possibly at local times outside the range of 08:00 to 13:00 LT reduced upward currents or downward currents could appear randomly and result in fainter emission along the main oval. Such decreases of the emission are occasionally formed along the main oval but are not observed frequently in many images implying a temporal origin rather than one fixed at a specific local time sector inferred by the magnetospheric plasma flows and current distribution of the Jovian magnetospheric system. An example of such a random decrease of the main oval emission can be seen in Figure 3 for the image taken at 158° CML. The emission drop is observed at  $\lambda_{III} \approx 195^\circ$ , which corresponds to the predawn sector. However, this drop is not as distinct as the discontinuity marked by the dashed lines and is not observed constantly in other images at a fixed magnetic local time. It could originate from an occasionally downward field-aligned current such as the one inferred by Pioneer 10.

#### 4. Summary and Conclusions

[28] The present study is based on the analysis of HST images obtained during the years 1997–2007. We report the

presence of a discontinuity in Jupiter's main oval. The emission along the main oval drops abruptly to less than 10% of the maximum emission, forming a discontinuity in the main oval. The feature is present in the north and south hemispheres. Images taken at different CML in both hemispheres show that the discontinuity appears fixed in magnetic local time. We magnetically map its position from the ionosphere to the equatorial plane, in order to investigate its origin. For the northern hemisphere the Ganymede footprint is also used as a reference for the magnetic mapping. The position of the discontinuity for both hemispheres is located in the prenoon sector. We perform a statistical analysis based on images in the north for the years 1997–2007. It is shown that the discontinuity is a frequently observed feature, along which the emission varies between 5 and 95 kR (with mean emission  $\sim 34$  kR) and its equatorial source is located between 08:00 and 13:00 LT.

[29] Pioneer and Voyager observations revealed the presence of reduced and reversed currents along the prenoon and predawn sectors, and upward currents along the midnight [Bunce and Cowley, 2001b]. These discrepancies were attributed to magnetospheric dynamics and alternatively to conductivity changes. From the close to zero field-aligned current along the Pioneer 11 pass (09:00 LT) we derive the precipitated energy flux in the ionosphere and we find it in very good agreement with the observed faint emissions along the discontinuity as derived by the statistical study (minimum emission of 5 to 95 kR with mean value  $\sim 34$  kR). Field-aligned current calculations based on Galileo measurements covering all local times, showed the existence of downward field-aligned currents in the near equatorial plane between 08:00 and 13:00 LT [Khurana, 2001]. The author argued that the current distributions are the result of the solar wind driven magnetospheric convection. Additionally, plasma flow measurements in the Jovian magnetosphere, inferred by Galileo [Krapp et al., 2001] show evidence of nearly corotating plasma in the dawn-to-dusk sector. According to theoretical studies [Cowley and Bunce, 2001, 2003; Cowley et al., 2003a, 2005] this would require weaker field-aligned currents (or reversed) and consequently fainter aurora emissions in the prenoon magnetic local time. Field-aligned current pattern in the near equatorial plane based on magnetohydrodynamic simulations [Walker and Ogino, 2003] confirmed the observations by predicting downward field-aligned currents in the prenoon and early afternoon local time sector in the near equatorial plane. It was additionally shown that field-aligned currents in the ionosphere predict an area of downward field-aligned currents in the region where the discontinuity is observed.

[30] In this work we report the presence of a discontinuity in Jupiter's main oval in both hemispheres, a feature frequently observed in the prenoon and early afternoon sector. We associate its origin with the reduced or/and downward field-aligned currents in that region, inferred by observations, theoretical considerations and magnetohydrodynamic simulations. We base our conclusions on the consistency of the location of its equatorial source with the location of the upward or/and reduced downward field-aligned currents. Finally, the precipitating energy flux in the ionosphere calculated for a typical reduced field-aligned

current at the location of the equatorial source of the discontinuity is found to be within the range of the observed faint emission.

[31] **Acknowledgments.** This work is based on observations with the NASA/ESA Hubble Space Telescope, obtained at the Space Telescope Science Institute (STScI), which is operated by AURA, inc. for NASA under contract NAS5-26555. The research was supported by the PRODEX Programme managed by the European Space Agency in collaboration with the Belgian Federal Science Policy Office and by the Belgian Fund for Scientific Research (FNRS).

[32] Wolfgang Baumjohann thanks the reviewers for their assistance in evaluating this paper.

## References

- Ballester, G. E., et al. (1996), Time-resolved observations of Jupiter's far-ultraviolet aurora, *Science*, *274*, 409–412.
- Bhattacharya, B., R. M. Thorne, and D. J. Williams (2001), On the energy source for diffuse Jovian auroral emissivity, *Geophys. Res. Lett.*, *14*, 2751–2754.
- Bonfond, B., J.-C. Gérard, D. Grodent, and J. Saur (2007), Ultraviolet Io footprint short timescale dynamics, *Geophys. Res. Lett.*, *34*, L06201, doi:10.1029/2006GL028765.
- Bunce, E. J., and S. W. H. Cowley (2001a), Local time asymmetry of equatorial current sheet in Jupiter's magnetosphere, *Planet. Space Sci.*, *49*, 261–274.
- Bunce, E. J., and S. W. H. Cowley (2001b), Divergence of the equatorial current in the dawn sector of Jupiter's magnetosphere: Analysis of Pioneer and Voyager magnetic field data, *Planet. Space Sci.*, *49*, 1089–1113.
- Clarke, J. T., et al. (1998), Hubble Space Telescope imaging of Jupiter's UV aurora during the Galileo orbiter mission, *J. Geophys. Res.*, *103*, 20,217–20,236.
- Clarke, J. T., et al. (2002a), Ultraviolet auroral emissions from the magnetic footprints of Io, Ganymede and Europa on Jupiter, *Nature*, *415*, 997–1000.
- Clarke, J. T., D. Grodent, and J. E. P. Connerney (2002b), The distorted shape of Jupiter's northern auroral oval-A possible magnetic anomaly, paper presented at the 34th Annual Meeting, Div. for Planet Sci., Birmingham, Ala., October.
- Connerney, J. E. P., M. H. Acuña, N. F. Ness, and T. Satoh (1998), New models of Jupiter's magnetic field constrained by the Io flux tube footprint, *J. Geophys. Res.*, *103*, 11,929–11,939.
- Cowley, S. W. H., and E. J. Bunce (2001), Origin of the main auroral oval in Jupiter's coupled magnetosphere-ionosphere system, *Planet. Space Sci.*, *49*, 1067–1088.
- Cowley, S. W. H., and E. J. Bunce (2003), Modulation of Jovian middle magnetosphere currents and auroral precipitation by solar wind-induced compressions and expansions of the magnetosphere: Initial response and steady state, *Planet. Space Sci.*, *51*, 31–56.
- Cowley, S. W. H., E. J. Bunce, and J. D. Nichols (2003a), Origins of Jupiter's main oval auroral emissions, *J. Geophys. Res.*, *108*(A4), 8002, doi:10.1029/2002JA009329.
- Cowley, S. W. H., E. J. Bunce, T. S. Stallard, and S. Miller (2003b), Jupiter's polar ionospheric flows: Theoretical interpretation, *Geophys. Res. Lett.*, *30*(5), 1220, doi:10.1029/2002GL016030.
- Cowley, S. W. H., I. I. Alexeev, E. S. Belenkaya, E. J. Bunce, C. E. Cottis, V. V. Kalegaev, J. D. Nichols, R. Prangé, and F. J. Wilson (2005), A simple axisymmetric model of magnetosphere-ionosphere coupling currents in Jupiter's polar ionosphere, *J. Geophys. Res.*, *110*, A11209, doi:10.1029/2005JA011237.
- Gérard, J.-C., D. Grodent, R. Prangé, J. H. Waite, G. R. Gladstone, V. Dols, F. Paresce, A. Storrs, L. Ben Jaffel, and K. A. Franke (1994), A remarkable aurora event on Jupiter observed in the ultraviolet with Hubble Space Telescope, *Science*, *266*, 1675–1678.
- Gérard, J.-C., A. Saglam, D. Grodent, and J. T. Clarke (2006), Morphology of the ultraviolet Io footprint emission and its control by Io's location, *J. Geophys. Res.*, *111*, A04202, doi:10.1029/2005JA011327.
- Grodent, D., J. T. Clarke, J. Kim, J. H. Waite Jr., and S. W. H. Cowley (2003a), Jupiter's main auroral oval observed with HST-STIS, *J. Geophys. Res.*, *108*(A11), 1389, doi:10.1029/2003JA009921.
- Grodent, D., J. T. Clarke, J. H. Waite Jr., S. W. H. Cowley, J.-C. Gérard, and J. Kim (2003b), Jupiter's polar auroral emissions, *J. Geophys. Res.*, *108*(A10), 1366, doi:10.1029/2003JA010017.
- Grodent, D., J.-C. Gérard, J. T. Clarke, G. R. Gladstone, and J. H. Waite Jr. (2004), A possible auroral signature of magnetotail reconnection process on Jupiter, *J. Geophys. Res.*, *109*, A05201, doi:10.1029/2003JA010341.
- Grodent, D., J.-C. Gérard, J. Gustin, B. H. Mauk, J. E. P. Connerney, and J. T. Clarke (2006), Europa's FUV auroral tail on Jupiter, *Geophys. Res. Lett.*, *33*, L06201, doi:10.1029/2005GL025487.

- Grodent, D., J.-C. Gérard, A. Radioti, B. Bonfond, A. Saglam (2008), Jupiter's changing auroral location, *J. Geophys. Res.*, *113*, A01206, doi:10.1029/2007JA012601.
- Gustin, J., J.-C. Gérard, D. Grodent, S. W. H. Cowley, J. T. Clarke, and A. Grad (2004), Energy-flux relationship in the FUV Jovian aurora deduced from HST-STIS spectral observations, *J. Geophys. Res.*, *109*, A10205, doi:10.1029/2003JA010365.
- Hill, T. W. (2001), The Jovian auroral oval, *J. Geophys. Res.*, *106*, 8101–8107.
- Khurana, K. K. (2001), Influence of the solar wind on Jupiter's magnetosphere deduced from currents in the equatorial plane, *J. Geophys. Res.*, *106*(A11), 25,999–26,016.
- Knight, S. (1973), Parallel electric fields, *Planet. Space Sci.*, *21*, 741.
- Krupp, N., A. Lagg, S. Livi, B. Wilken, J. Woch, E. C. Roelof, and D. J. Williams (2001), Global flows of energetic ions in Jupiter's equatorial plane: First-order approximation, *J. Geophys. Res.*, *106*, 26,017–26,032.
- Nichols, J. D., and S. W. H. Cowley (2004), Magnetosphere-ionosphere coupling currents in Jupiter's middle magnetosphere: Effect of precipitation-induced enhancements of the Pedersen conductivity, *Ann. Geophys.*, *22*, 1799–1827.
- Southwood, D. J., and M. G. Kivelson (2001), A new perspective concerning the influence of the solar wind in the Jovian magnetosphere, *J. Geophys. Res.*, *106*, 6123–6130.
- Tomás, A. T., J. Woch, N. Krupp, A. Lagg, K.-H. Glassmeier, and W. S. Kurth (2004), Energetic electrons in the inner part of the Jovian magnetosphere and their relation to auroral emissions, *J. Geophys. Res.*, *109*, A06203, doi:10.1029/2004JA010405.
- Waite, J. H., Jr., et al. (2001), An auroral flare at Jupiter, *Nature*, *410*, 787–789.
- Walker, R. J., and T. Ogino (2003), A simulation study of currents in the Jovian magnetosphere, *Planet. Space Sci.*, *51*, 295–307.
- 
- B. Bonfond, J.-C. Gérard, D. Grodent, and A. Radioti, LPAP, Institut d'Astrophysique et de Géophysique, Université de Liège, Belgium. (a.radioti@ulg.ac.be)
- N. Krupp and J. Woch, Max-Planck-Institut für Sonnensystemforschung, Katlenburg-Lindau, Germany.